

Effect of Boundary Layers on Solid Walls in Three-Dimensional Subsonic Wind Tunnels

Jerry B. Adcock* and Richard W. Barnwell†
NASA Langley Research Center, Hampton, Virginia

A solution for the solid blockage and lift interference caused by the boundary layers on solid walls in subsonic wind tunnels is presented. This solution results from a linear treatment similar to that for wind tunnels ventilated with longitudinal slots. The dynamics of the boundary layer is modeled with the von Kármán momentum-integral equation. The analysis leads to a viscous boundary condition which is a linear function of the inviscid velocity potential and enters the solution only as a change in boundary condition for the inviscid solution. The wall boundary layer primarily affects the solid blockage and streamline curvature interference factors, with the viscous layer reducing solid blockage in a manner similar to opening longitudinal slots in the walls.

Introduction

A NUMBER of linear methods have been developed for predicting the interference of open, closed, and ventilated walls in two- and three-dimensional subsonic wind tunnels. Summaries and applications of these methods are given in Refs. 1-3. In general, the ventilated walls are assumed to be homogeneous and are either perforated with small holes or slotted longitudinally. The purpose of the present paper is to present a linear method that accounts for the effects of boundary layers on solid walls in subsonic three-dimensional wind tunnels. As will be shown, the numerical method and the nature of the results bear a striking resemblance to those for subsonic wind tunnels with slotted walls.

The critical feature of the present method is the manner in which the boundary condition for solid wind tunnel walls is handled. The present method is based on a theory developed recently by Barnwell⁴ and Sewall⁵ which predicts the effects of boundary layers on solid sidewalls in two-dimensional subsonic and transonic wind tunnels. In this theory, the streamwise gradient of the displacement thickness for a solid-wall boundary layer is expressed in terms of the von Kármán momentum integral. Because the effective Reynolds number for the boundary layer on a wind tunnel wall at the model station is very large, the growth of the boundary layer due to the wall shearing stress is small compared to the variation caused by the model-induced pressure gradient. As a result, the viscous boundary condition can be expressed in terms of the edge velocity gradient and, hence, the gradient of the inviscid velocity potential function at the wall. This means that viscous and inviscid solutions do not have to be interacted and that the viscous solution can be obtained from the completed inviscid solution with this modified wall boundary condition.

The present solution for three-dimensional flow is substantially different from the two-dimensional solutions of Refs. 4 and 5 in that the two-dimensional solutions result in similarity rules relating compressibility and sidewall boundary-layer effects. No such similarity exists for the three-dimensional problem.

It is noted that the wall/boundary layer interaction problem has been studied previously by Berndt⁶ and Lofgren⁷ for transonic flow past models in closed three-dimensional wind

tunnels. However, the treatments in these references do not employ the von Kármán momentum integral formulation used in the present method.

Boundary-Layer Analysis

Consider steady subsonic, small perturbation flow in a wind tunnel with a rectangular cross section of width $2b$ and height $2h$ (Fig. 1). Let the Cartesian coordinates in the freestream, horizontal, and vertical directions be x , y , and z , respectively, and let the perturbation velocity potential be ϕ . The boundary condition at solid wind tunnel walls is

$$\frac{\partial \phi}{\partial n} = -U_e \frac{\partial \delta^*}{\partial x} \quad (1)$$

where n is the coordinate normal to the tunnel wall and positive outward, and U_e and δ^* are the boundary-layer edge velocity and displacement thickness.

In the present treatment, the dynamics of the sidewall boundary layer are modeled with the von Kármán momentum integral, which can be written as

$$\frac{\partial \delta^*}{\partial x} = -\frac{\delta^*}{U_e} (2 + H - M_e^2) \frac{\partial U_e}{\partial x} + \frac{\delta^*}{H} \frac{\delta H}{\delta x} + \frac{\tau_w}{\rho_e U_e^2} \quad (2)$$

where ρ_e and M_e are the density and Mach number at the boundary-layer edge, and H and τ_w are the boundary-layer shape factor and surface shearing stress. For the present problem, Eq. (2) can be simplified because the sidewall boundary layer in most wind tunnels can be approximated as a flat-plate boundary layer with a large Reynolds number and an equivalent length of the order of $\delta^*/(\tau_w/\rho_e U_e^2)$. In general, the model length scale c is much smaller than the boundary-layer equivalent length, so that the inequality

$$\frac{\tau_w}{\rho_e U_e^2} \ll \frac{\delta^*}{c} \quad (3)$$

applies, and, as a result, the last term in Eq. (2) can be neglected in the first approximation. As shown in Ref. 8, the shape factor for boundary layers with constant total temperatures can be approximated as

$$H = (\bar{H} + 1) \left(1 + \frac{\gamma - 1}{2} M^2 \right) - 1 \quad (4)$$

where \bar{H} is the transformed shape factor and γ is the ratio of specific heats. Because \bar{H} approaches one as the Reynolds

Presented as Paper 83-0144 at the AIAA 21st Aerospace Sciences Meeting, Reno, Nev., Jan. 10-13, 1983; submitted March 8, 1983; revision received June 23, 1983. This paper is declared a work of the U.S. Government and therefore is in the public domain.

*Aeronautical Engineer. Member AIAA.

†Head, NTF Aerodynamics Branch. Associate Fellow AIAA.

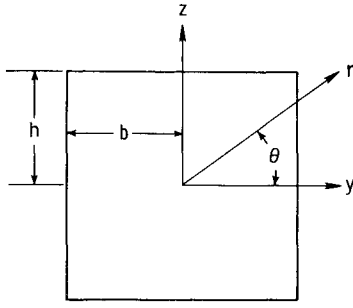


Fig. 1 Wind tunnel cross section and coordinates.

number becomes large, Eq. (4) can be written as

$$H = 1 + (\gamma - 1)M^2 \quad (5)$$

for the present problem. From Eq. (5) and the small perturbation energy equation, it follows that

$$\frac{\partial H}{\partial x} = \frac{(H-1)(H+1)}{U_e} \frac{\partial U_e}{\partial x} \quad (6)$$

With inequality (3) and Eq. (6), Eq. (2) can be written as

$$\frac{\partial \delta^*}{\partial x} = -\frac{\delta^*}{U_e} \left(2 + \frac{1}{H} - M_e^2 \right) \frac{\partial U_e}{\partial x} \quad (7)$$

It should be noted that the present theory does not actually require that the last term in Eq. (2) be negligible. This term is effectively removed in many wind tunnels by simply sloping the walls outward to account for the flat-plate growth of the wall boundary layer. Including the term would have no effect on the basic results of the present paper.

With Eq. (7), boundary condition (1) can be written for subsonic flow as

$$\frac{\partial \phi}{\partial \bar{n}} = \frac{\delta^*}{b} \left(1 + \frac{1+H}{\beta^2 H} \right) \frac{\partial^2 \phi}{\partial \bar{x}^2} \quad (8)$$

where

$$\beta = \sqrt{1 - M_\infty^2} \quad (9)$$

and $\bar{n} = n/b$ and $\bar{x} = x/\beta b$ are nondimensional incompressible coordinates. For small disturbance flow, the quantities H and δ^* in Eq. (8) can be approximated by representative constant values such as those at the model station in the empty tunnel.^{4,5} Then the boundary layer is a linear function of the inviscid perturbation velocity potential. In this approximation, the dependence on viscosity is expressed entirely with nonvarying parameters, and the viscous boundary condition can be incorporated in the classical linear wall interference problem.

Equation (8) is similar in form to the conventional linear boundary conditions for slotted and porous walls, which are written as

$$\frac{\partial \phi}{\partial \bar{n}} + \frac{1}{F} \phi = 0 \quad (10)$$

and

$$\frac{\partial \phi}{\partial \bar{n}} + \frac{R}{\beta} \frac{\partial \phi}{\partial \bar{x}} = 0 \quad (11)$$

respectively, where F and R are nondimensional constants. It will be shown that the potential flow solutions obtained with Eq. (7) for the viscous solid wall boundary conditions are very

similar to those with Eq. (10) for the slotted wall boundary condition.

Basic Potential Flow Formulation

A classical linear wall-interference problem is solved with the method which Pindzola and Lo¹ applied to the slotted-wall problem. Subsonic flow is governed by Laplace's equation, which is written in cylindrical polar incompressible coordinates (Fig. 1) as

$$\beta^2 \frac{\partial^2 \phi}{\partial x^2} + \frac{\partial^2 \phi}{\partial r^2} + \frac{1}{r} \frac{\partial \phi}{\partial r} + \frac{1}{r^2} \frac{\partial^2 \phi}{\partial \theta^2} = 0 \quad (12)$$

The solution is assumed to be of the form

$$\phi = \phi_m + \phi_i \quad (13)$$

where ϕ_m is the perturbation potential caused by a model in free air, and ϕ_i the interference potential induced by wind tunnel walls. Linear superposition is used to construct representations of ϕ_m and ϕ_i .

Model Potential Representation

Simple singularities are used for the model potentials. A doublet is used to represent the solid blockage due to model volume as

$$\phi_{m1} = \frac{\mu_s}{4\pi} \frac{x}{(x^2 + \beta^2 r^2)^{3/2}} \quad (14)$$

where $\mu_s = U_\infty \tau$, and τ is the model volume. A horseshoe vortex with infinitesimal width is used to represent the model lift as

$$\phi_m = \phi_{m2} + \phi_{m3} = \frac{\Gamma s \sin \theta}{2\pi} \frac{1}{r} + \frac{\Gamma s}{2\pi} \frac{x}{(x^2 + \beta^2 r^2)^{1/2}} \frac{\sin \theta}{r} \quad (15)$$

where Γ is the circulation and s the wing semispan. Subscripts 2 and 3 indicate "two-dimensional" (r, θ) and "three-dimensional" (x, r, θ) solutions.

Following Pindzola and Lo,¹ Fourier sine transforms are used for the solid blockage and "three-dimensional" lift potentials. This transformation is written as

$$\phi(x, r, \theta) = \sqrt{\frac{2}{\pi}} \int_0^\infty \bar{\phi}(r, \theta, q) \sin\left(\frac{qx}{\beta b}\right) dq \quad (16)$$

$$\bar{\phi}(r, \theta, q) = \sqrt{\frac{2}{\pi}} \int_0^\infty \phi(x, r, \theta) \sin\left(\frac{qr}{\beta b}\right) \frac{dx}{\beta b} \quad (17)$$

Note that no Fourier transform is needed for the "two-dimensional" lift potential because it is independent of the coordinate x . The Fourier transform for the solid blockage is

$$\bar{\phi}_{m1} = \sqrt{\frac{2}{\pi}} \frac{q \mu_s}{4\pi \beta^2 b^2} K_0\left(\frac{qr}{b}\right) \quad (18)$$

where $K_0(qr/b)$ is the modified Bessel function of second kind of order zero.

The Fourier transform for the "three-dimensional" lift interference is

$$\bar{\phi}_{m3} = \sqrt{\frac{2}{\pi}} \frac{\Gamma s}{2\pi \beta b} \sin \theta K_1\left(\frac{qr}{b}\right) \quad (19)$$

where $K_1(qr/b)$ is the modified Bessel function of second kind of order one.

Interference Potential Representation

Now consider the solid blockage interference. Because this phenomenon is symmetric about both the horizontal and

vertical planes, the transform function can be written as

$$\bar{\phi}_{il}(r, \theta, q) = \sum_{m=0,2,4}^{\infty} R_m(r, q) \cos m\theta \quad (20)$$

With Eqs. (12), (16), and (20), it is found that the governing equation for R_m is

$$\frac{d^2 R_m}{dr^2} + \frac{1}{r} \frac{dR_m}{dr} - \left(\frac{m^2}{r^2} + \frac{q^2}{b^2} \right) R_m = 0 \quad (21)$$

The solutions to this equation are modified Bessel functions. The general solution for ϕ_{il} is

$$\bar{\phi}_{il}(r, \theta, q) = C_1 \sum_{m=0,2,4}^{\infty} A_m(q) I_m\left(\frac{qr}{b}\right) \cos m\theta \quad (22)$$

where $I_m(qr/b)$ is the modified Bessel function of first kind of order m , and

$$C_1 = \sqrt{\frac{2}{\pi}} \frac{\mu_s}{4\pi\beta^2 b^2} q$$

The phenomenon of lift interference is asymmetric about the horizontal plane and symmetric about the vertical plane. With an analysis similar to the one above it can be shown that the "three-dimensional" lift interference transform function can be written as

$$\bar{\phi}_{i3}(r, \theta, q) = C_3 \sum_{m=1,3,5}^{\infty} B_m(q) I_m\left(\frac{qr}{b}\right) \sin m\theta \quad (23)$$

where

$$C_3 = \sqrt{\frac{2}{\pi}} \frac{\Gamma_s}{2\pi b}$$

The "two-dimensional" lift solution does not require a transformation. The interference potential ϕ_{i2} can be written as

$$\phi_{i2}(r, \theta) = C_2 \sum_{m=1,3,5}^{\infty} D_m r^m \sin m\theta \quad (24)$$

where

$$C_2 = \Gamma_s / 2\pi b$$

Boundary Condition Representation

The transformed boundary condition for the solid blockage and "three-dimensional" lift interference for a solid wall with boundary layer is

$$\frac{\partial}{\partial \bar{n}} (\bar{\phi}_{mj} + \bar{\phi}_{ij}) + q^2 \frac{\delta^*}{b} \left(1 + \frac{1+H}{\beta^2 H} \right) (\bar{\phi}_{mj} + \bar{\phi}_{ij}) = 0 \quad j=1 \text{ and } 3 \quad (25)$$

For a slotted wall, the boundary condition is

$$\frac{\partial}{\partial \bar{n}} (\bar{\phi}_{mj} + \bar{\phi}_{ij}) + \frac{1}{F} (\bar{\phi}_{mj} + \bar{\phi}_{ij}) = 0, \quad j=1 \text{ and } 3 \quad (26)$$

The boundary conditions for the "two-dimensional" lift solutions for these two problems are

$$\frac{\partial}{\partial \bar{n}} (\phi_{m2} + \phi_{i2}) = 0 \quad (27)$$

and

$$\frac{\partial}{\partial \bar{n}} (\phi_{m2} + \phi_{i2}) + \frac{1}{F} (\phi_{m2} + \phi_{i2}) = 0 \quad (28)$$

Equations (25-28) can be evaluated using Eqs. (15), (18), (19), and (22-24). The resulting equations are used to evaluate the coefficients $A_m(q)$, $B_m(q)$, and D_m in Eqs. (22-24).

The new forms of the boundary conditions are given in the Appendix. In practice, the infinite series is truncated, and the resulting approximate forms are evaluated at a sufficient number of points on the wind tunnel wall. In the present treatment, these points are chosen at evenly spaced intervals of wall length from $\theta = 0$ to $\pi/2$.

Solid Blockage Interference

In Ref. 1, it is shown that the streamwise velocity induced at the model station by the wind tunnel walls in the presence of the model can be obtained from Eqs. (16) and (2) as

$$u_s(0,0) = \frac{\partial \theta_i}{\partial x} \Big|_{r=0}^{x=0} = \frac{U_\infty \tau}{2\pi^2 \beta^3 b^3} \int_0^\infty A_0(q) q^2 dq \quad (29)$$

With Eq. (16), it can be shown that the gradient of this model-induced interference velocity at the model station is

$$\frac{\partial u_s(0,0)}{\partial x} = 0 \quad (30)$$

It is customary to present solid blockage in terms of the blockage ratio

$$\Omega = \frac{u_s(0,0)}{U_{s,c}(0,0)} \quad (31)$$

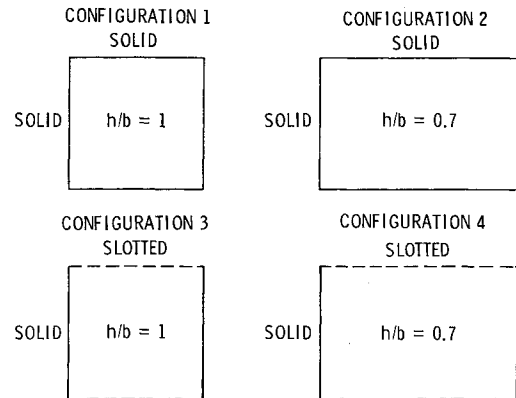


Fig. 2 Wind tunnel configurations.

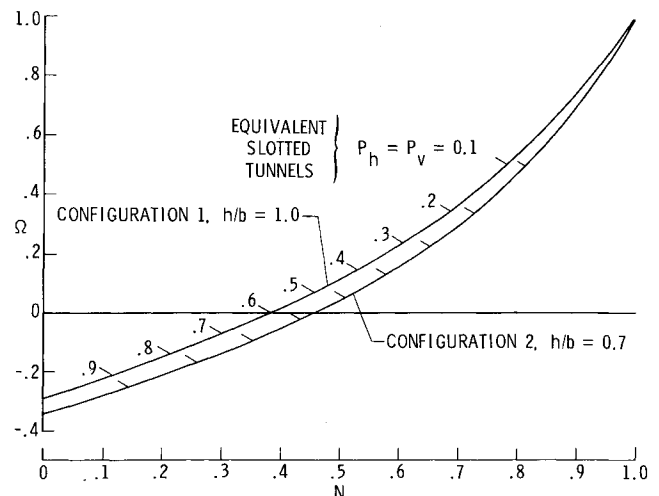


Fig. 3 Solid blockage ratio for solid-wall tunnel configurations at the model position ($x=0$).

where $u_{s,c}$ is the blockage for the closed-wall configuration with the wall ratio h/b . For wind tunnels with $h/b = 1$ and 0.7 , the quantity $2\pi^2\beta^3b^3u_{s,c}(0,0)/U_\infty\tau$ has the values of 1.7717 and 3.2213, respectively.

In the present treatment, the slotted-wall results are presented in terms of the parameter P of Ref. 1, which is related to the slotted-wall coefficient F by the expression

$$P = 1/(1+F) \quad (32)$$

This parameter has values of 0 and 1 for closed and open walls, respectively. The results for solid walls with boundary layers will be presented in terms of the parameter

$$N = 1/\left\{1 + \frac{\delta^*}{b} \left[1 + \frac{1+H}{\beta^2 H}\right]\right\} \quad (33)$$

This parameter has a value of 1 for a wall with a zero-thickness boundary layer. As a study of the boundary conditions will show, the blockage for a solid wall with $N=1$ and a slotted wall with $P=0$ must be identical because both are simply a solid wall with no boundary layer. Although it is not as obvious, the boundary conditions require that the blockage for a solid wall with $N=0$ be identical to a slotted wall with $P=1$. The solid wall with a value of N near zero is simply a solid wall with a boundary layer and a near-sonic freestream velocity.

Lift Interference

The wall-induced upwash along the wind tunnel axis ($r=0$) can be obtained from the lift-interference potential as

$$w = \frac{\partial\phi_i}{\partial z} \Big|_{r=0} = \frac{\Gamma S}{2\pi b} \left(D_l + \frac{1}{\pi b} \int_0^\infty B_l(q) \sin\left(\frac{qx}{\beta b}\right) q dq \right) \quad (34)$$

As in Ref. 1, the lift interference and streamline curvature factors are expressed as

$$\delta = \left(\frac{4bh}{SC_L} \right) \frac{w}{U_\infty} \quad (35)$$

and

$$\delta_l = \frac{8\beta b h^2}{SC_L} \left(\frac{1}{U_\infty} \frac{\partial w}{\partial x} \right) \quad (36)$$

where S is the model reference area and C_L the lift coefficient.

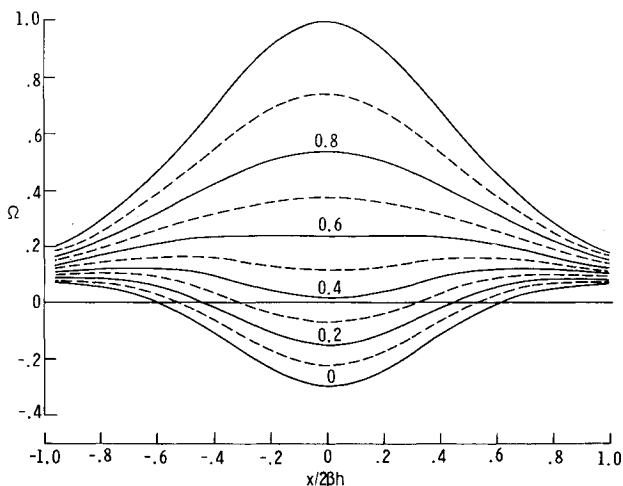


Fig. 4 Distributions of solid blockage ratio along axis of configuration 1.

The lift interference factor at the model station is

$$\delta_0 = (h/2\pi) D_l \quad (37)$$

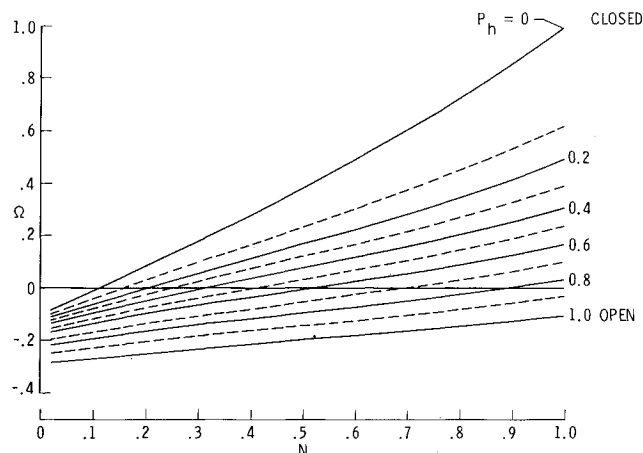
and the streamline curvature factor at the model station is

$$\delta_l = \frac{h^2}{\pi^2 b^2} \int_0^\infty B_l(q) q^2 dq \quad (38)$$

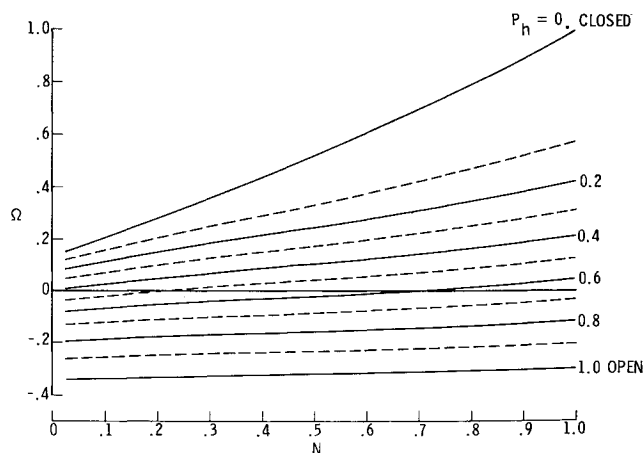
From an examination of the boundary conditions, it can be seen that the streamline curvature factor δ_l , which is a function only of the "three-dimensional" lift solution, is the same for a slotted wall with $P=0$ and a solid wall with $N=1$ and also for a slotted wall with $P=1$ and a solid wall with $N=0$. The lift interference factor at the model station, δ_0 , involves only the "two-dimensional" lift solution and does not depend on the parameter N . Lift interference for all values of the boundary-layer thickness is the same as that for a closed wall with no boundary layer. This is the same as the slotted wall solution with $P=0$.

Results

Results are presented for the four rectangular wind tunnel configurations depicted in Fig. 2. These configurations include tunnels with four solid walls with boundary layers, and tunnels with solid sidewalls with boundary layers and slotted upper and lower walls. Cross-sectional aspect ratios of $h/b = 1$ and 0.7 are treated.



a) Configuration 3, $h/b = 1.0$.



b) Configuration 4, $h/b = 0.7$.

Fig. 5 Solid blockage ratio for combination-wall configurations at the model position ($x=0$).

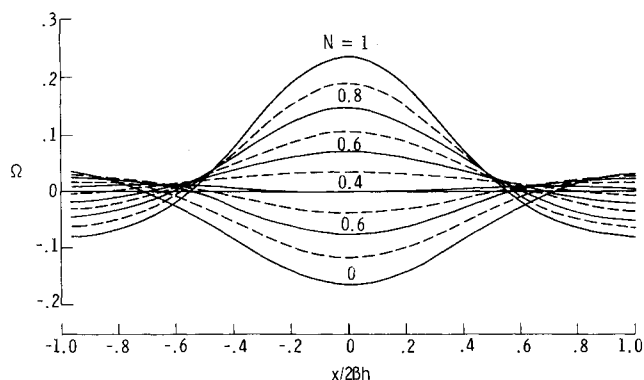


Fig. 6 Distributions of solid blockage ratio along axis of configuration 3, $P_h = 0.5$.

Solid Blockage Interference

The model-induced wall boundary-layer effects on the solid blockage for the solid-wall configurations 1 and 2 are presented in Fig. 3. These blockage ratios, Ω , are at the model position ($x=0$) and for values of the boundary-layer parameter, N , from 0.0 to 1.0. In reality, values of N less than about $\frac{2}{3}$ are largely academic because they can be obtained only with excessively thick boundary layers or with near-sonic freestream Mach numbers; in both cases, this linear procedure would be less than adequate for the problem. The model-induced wall boundary-layer effect reduces the blockage factor from the closed-wall zero-thickness value ($N=1$, $\Omega=1$) and is similar to the blockage relief that is obtained when the walls are slotted. As a matter of interest, the tick marks indicate the slot parameter values for an equivalent slotted tunnel ($P=P_h=P_v$ on horizontal and vertical walls) that would produce the same blockage factors. For the square tunnel, a boundary-layer parameter, N , of 0.780 produced a blockage ratio of 0.5 as does the slotted tunnel with a P factor of 0.1. For given boundary-layer parameter values, the blockage relief is greater for configuration 2 ($h/b=0.7$) than for the square tunnel.

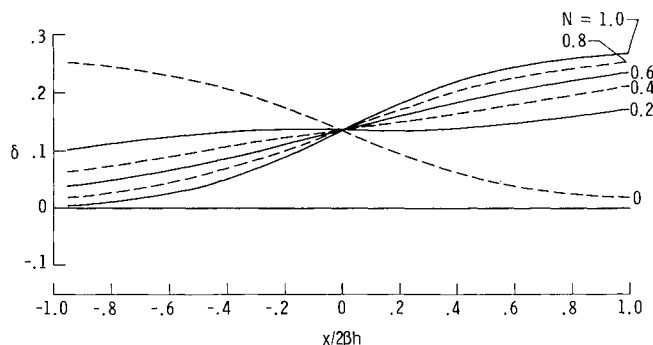
The wall boundary-layer effect on the solid blockage distribution along the longitudinal axis of the tunnel configuration 1 has been evaluated and is shown in Fig. 4. The blockage factor varies symmetrically about the model position with N values from 0.4 to 0.6 producing fairly constant values of blockage along the axis.

The wall boundary-layer effects on the blockage factors for the combination wall tunnel configurations (3 and 4) are presented in Figs. 5 and 6. For these configurations, it is assumed that the horizontal wall boundary condition is dominated by the slot effects; no attempt has been made to combine slot and boundary-layer boundary conditions on the same wall. The blockage factors at the model position are shown in Figs. 5a and 5b. At $N=1.0$ (no sidewall boundary layers), the blockage factors for the various horizontal slot parameter values are the same as those of Pindzola and Lo.¹ As the boundary layer on the sidewall builds up (decreasing N), additional blockage-ratio reductions occur. This effect is more pronounced for the more closed horizontal slots. As the horizontal slots go toward fully open ($P_h=1.0$), it is anticipated that the sidewall boundary-layer effect should diminish.

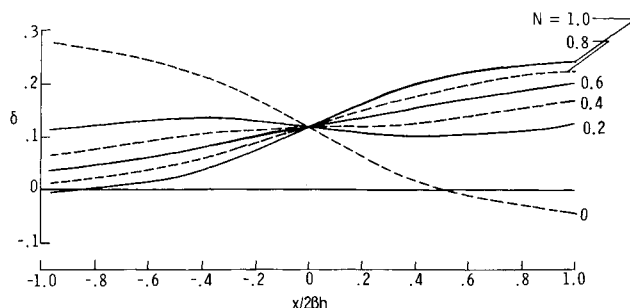
The boundary-layer effect on the blockage along the longitudinal axis of tunnel configuration 3 with a horizontal slot factor of 0.5 is presented in Fig. 6.

Lift Interference

The lift interference, δ , defined by Eqs. (34) and (35), contains two terms, one of which is independent of x (two-dimensional lift) and the second of which is x -dependent



a) Configuration 1, $h/b = 1.0$.



b) Configuration 2, $h/b = 0.7$.

Fig. 7 Distributions of lift interference factor along axis of solid-wall tunnel configurations.

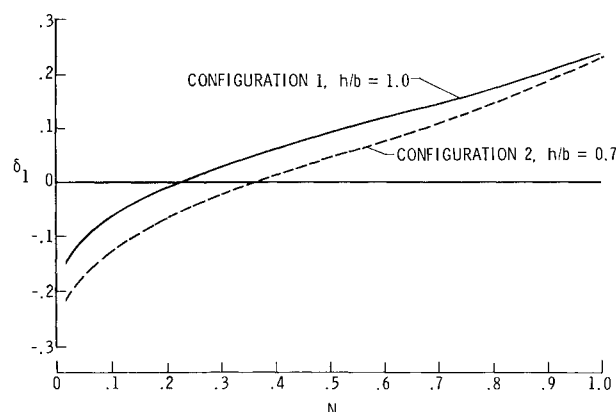


Fig. 8 Streamline curvature factor for solid-wall tunnel configurations at the model position ($x=0$).

(three-dimensional lift). An examination of the two-dimensional lift boundary condition [Eq. (27)] reveals that the wall boundary-layer parameter, N , has no effect on the two-dimensional lift interference term. The value for this term is just the closed-wall value. The three-dimensional lift term is affected by the wall boundary layer; the longitudinal distributions of this term for the solid-wall tunnel configurations are shown in Fig. 7. The lift interference values for the no-boundary-layer case ($N=1$) are the same as those of Ref. 1. It is apparent that the effect of the wall boundary layer is smaller for the lift interference factor than for the solid blockage ratio.

The model-induced wall boundary layer effects on the streamline curvature factor δ_1 for the various tunnel configurations are presented in Figs. 8-10. For the solid-wall configurations (Figs. 8 and 9), the streamline curvature factors near the model station ($x=0$) are reduced by the wall boundary-layer effect. This effect is similar to opening slots in

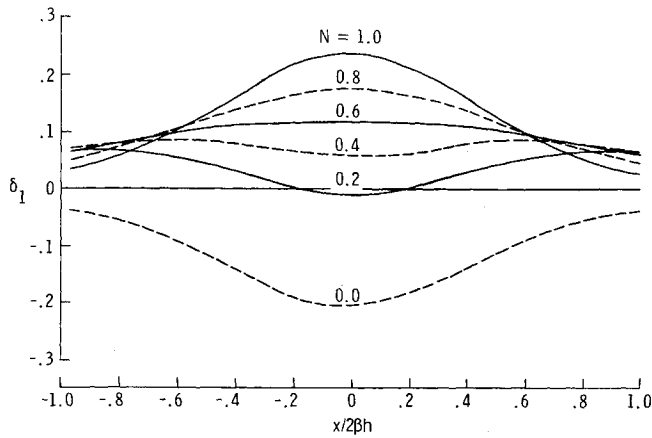
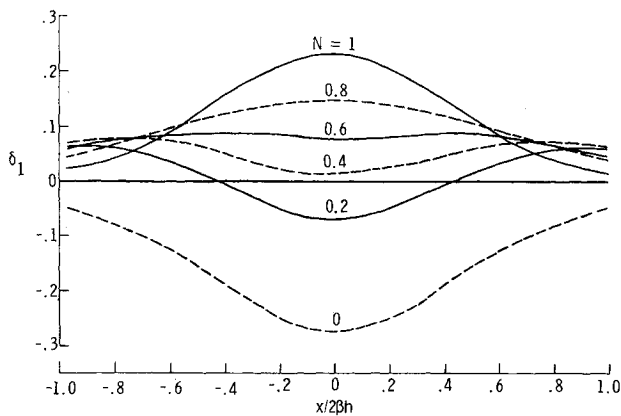
a) Configuration 1, $h/b = 1.0$.b) Configuration 2, $h/b = 0.7$.

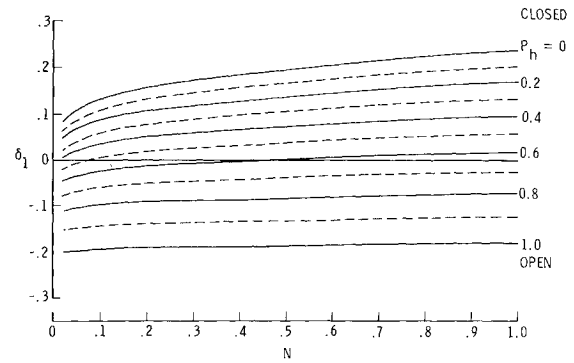
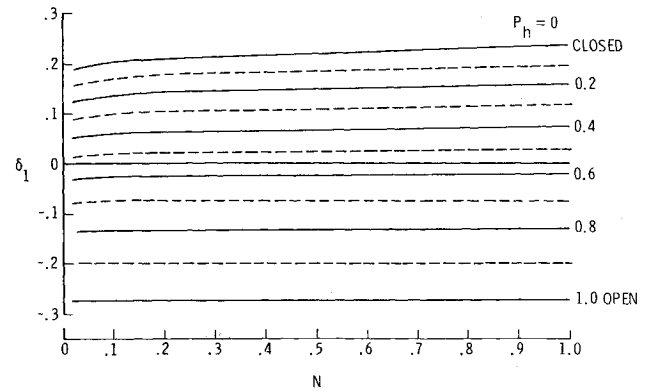
Fig. 9 Distributions of streamline-curvature factor along axis of solid-wall tunnel configurations.

the horizontal walls (see Fig. 10). For these combination wall configurations, the slotted horizontal wall effects are dominant with only slight changes in the streamline curvature factor for practical values of the boundary-layer parameter N .

Concluding Remarks

A solution for the tunnel wall boundary-layer effects for three-dimensional subsonic tunnels has been presented. The fundamentals and methodology of the procedure are the same as the Pindzola and Lo¹ treatment of the ventilated wall problem. The model potentials are represented with simple singularities placed on the centerline of the tunnel and Laplace's equation in cylindrical coordinates is solved for either conventional homogeneous slotted-wall boundary condition or the solid-wall viscous boundary condition,^{4,5} or a combination of them. The Fourier transform and point matching technique of Ref. 1 are used.

The solid-wall, viscous boundary condition is the result of modeling the dynamics of the boundary layer with the von Kármán momentum-integral equation and assuming that both the Reynolds number of the flow and the distance to the model station are very large so that the growth of the boundary layer is very small. This leads to an approximate viscous boundary condition that is a linear function of the inviscid perturbation velocity potential. The viscous wall effects enter the problem only as a change in boundary condition for the inviscid solution. For analysis purposes, a viscous boundary parameter somewhat analogous to the slot parameter P of Pindzola and Lo¹ is established. New forms of

a) Configuration 3, $h/b = 1.0$.b) Configuration 4, $h/b = 0.7$.Fig. 10 Streamline curvature factors for combination-wall tunnel configurations at the model position ($x = 0$).

the boundary condition equations for viscous-wall and slotted-wall solutions are presented in the Appendix.

This analysis of the model-induced boundary-layer effects on the solid walls of several three-dimensional wind tunnel configurations leads to the following observations.

1) The most pronounced wall boundary-layer effect is on solid blockage for completely closed wind tunnels. Boundary layers on the wall reduce the blockage from the solid-wall, no-boundary-layer case in a manner similar to opening slots in a solid wall.

2) Additionally, for solid-wall tunnel configurations, the streamline curvature interference factor is reduced by a significant amount, whereas the lift interference factor at the model station does not depend on the boundary-layer parameter.

3) For combination wall configurations, the slot effect of the horizontal walls dominates the viscous effect on the solid sidewalls. This is true not only for solid blockage but for lift and streamline curvature interference as well.

Appendix—Boundary Conditions

The boundary conditions for solid walls with boundary layers and slotted walls are given in this Appendix. The conditions for solid blockage are

$$\begin{aligned} \sum_{m=0,2,4}^{\infty} A_m(q) \left(Dq^n I_m \left(\frac{qr}{b} \right) \cos m\theta \pm E \cos \theta \right. \\ \left. \times \left[q I_{m+1} \left(\frac{qr}{b} \right) \cos m\theta + m I_m \left(\frac{qr}{b} \right) \cos [(m-1)\theta] \right] \right) \\ = -Dq^n K_0 \left(\frac{qr}{b} \right) \pm Eq \cos \theta K_1 \left(\frac{qr}{b} \right), \quad y = \pm b \quad (A1) \end{aligned}$$

$$\begin{aligned}
& \sum_{m=0,2,3}^{\infty} A_m(q) \left(Dq^n I_m \left(\frac{qr}{b} \right) \cos m\theta \pm E \sin \theta \right. \\
& \times \left[q I_{m+1} \left(\frac{qr}{b} \right) \cos m\theta - m \frac{b}{h} I_m \left(\frac{qr}{b} \right) \sin([m-1]\theta) \right] \Big) \\
& = -Dq^n K_0 \left(\frac{qr}{b} \right) \pm E q \sin \theta K_1 \left(\frac{qr}{b} \right), \quad z = \pm h \quad (A2)
\end{aligned}$$

where

$$D = \frac{\delta^*}{b} \left(1 + \frac{1+H}{\beta^2 H} \right), \quad E=1, \quad n=2$$

for solid walls with boundary layers and

$$D=1, \quad E=F(h/b), \quad n=0$$

for slotted walls.

The boundary conditions for the "three-dimensional" lift solution are

$$\begin{aligned}
& \sum_{m=1,3,5}^{\infty} B_m(q) \left(Dq^n I_m \left(\frac{qr}{b} \right) \sin m\theta \pm E \cos \theta \right. \\
& \times \left[q I_{m+1} \left(\frac{qr}{b} \right) \sin m\theta + m I_m \left(\frac{qr}{b} \right) \sin([m-1]\theta) \right] \Big) \\
& = -\sin \theta \left(Dq^n K_1 \left(\frac{qr}{b} \right) \mp E q \cos \theta K_2 \left(\frac{qr}{b} \right) \right), \quad y = \pm b \quad (A3)
\end{aligned}$$

$$\begin{aligned}
& \sum_{m=1,3,5}^{\infty} B_m(q) \left(Dq^n I_m \left(\frac{qr}{b} \right) \sin m\theta \pm E \sin \theta \right. \\
& \times \left[q I_{m+1} \left(\frac{qr}{b} \right) \sin m\theta + m \frac{b}{h} I_m \left(\frac{qr}{b} \right) \cos([m-1]\theta) \right] \Big) \\
& = -\sin \theta \left(Dq^n K_1 \left(\frac{qr}{b} \right) \pm E \left[\frac{b}{h} K_1 \left(\frac{qr}{b} \right) \right. \right. \\
& \left. \left. - q \sin \theta K_2 \left(\frac{qr}{b} \right) \right] \right), \quad z = \pm h \quad (A4)
\end{aligned}$$

where D , E , and n are defined as before.

The boundary conditions for the "two-dimensional" lift solutions are

$$\begin{aligned}
& \sum_{m=1,3,5}^{\infty} D_m r^m \left(\sin m\theta \pm E \frac{h}{b} m \cos \theta \sin([m-1]\theta) \right) \\
& = -\sin \theta \cos \theta \left(1 - 2E \frac{h}{b} \cos^2 \theta \right), \quad y = \pm b \quad (A5)
\end{aligned}$$

$$\begin{aligned}
& \sum_{m=1,3,5}^{\infty} D_m r^m \left(\sin m\theta \pm E m \sin \theta \cos([m-1]\theta) \right) \\
& = -\frac{b}{h} \sin^2 \theta (1 + E \cos 2\theta), \quad z = \pm h \quad (A6)
\end{aligned}$$

where $1/E=0$ for solid walls with boundary layers and $E=F$ for slotted walls.

References

- ¹Pindzola, M. and Lo, C. F., "Boundary Interference at Subsonic Speeds in Wind Tunnels with Ventilated Walls," AEDC-TR-69-47, May 1969.
- ²Lo, C. F. and Oliver, R. H., "Subsonic Lift Interference in a Wind Tunnel with Perforated Walls," *Journal of Aircraft*, Vol. 7, March 1970, pp. 281-283.
- ³Garner, H. C., Rogers, E. W. E., Acum, W. E. A., and Maskell, E. C., "Subsonic Wind-Tunnel Wall Corrections," AGARDograph 109, Oct. 1966.
- ⁴Barnwell, R. W., "Similarity Rule for Sidewall Boundary-Layer Effect in Two-Dimensional Wind Tunnels," *AIAA Journal*, Vol. 18, Sept. 1980, pp. 1149-1151.
- ⁵Sewall, W. G., "Effects of Sidewall Boundary Layers in Two-Dimensional Subsonic and Transonic Wind Tunnels," *AIAA Journal*, Vol. 20, Sept. 1982, pp. 1253-1256.
- ⁶Berndt, S. B., "On the Influence of Wall Boundary Layers in Closed Transonic Test Sections," FAA Rept. 71, 1957.
- ⁷Lofgren, P., "Simplification of the Boundary Condition at a Slotted Wind-Tunnel Wall with a Boundary Layer," FFA Tech. Note AV-932, March 1975.
- ⁸Green, J. E., "Interactions Between Shock Waves and Turbulent Boundary Layers," *Progress in Aeronautical Sciences*, Vol. II, Pergamon Press, New York, 1970, pp. 269-270.